

ResQ: Mixed-Precision Quantization of Large Language Models with Low-Rank Residuals

Utkarsh Saxena¹ Sayeh Sharify², Kaushik Roy¹, Xin Wang²

¹Department of Electrical and Computer Engineering, Purdue University

²d-Matrix, Santa Clara, USA

¹{saxenau, kaushik}@purdue.edu, ²{sayehs, xwang}@d-matrix.ai

Abstract

Post-training quantization (PTQ) of large language models (LLMs) holds the promise in reducing the prohibitive computational cost at inference time. Quantization of all weight, activation and key-value (KV) cache tensors to 4-bit without significantly degrading generalizability is challenging, due to the high quantization error caused by extreme outliers in activations. To tackle this problem, we propose *ResQ*, a PTQ method that pushes further the state-of-the-art. By means of principal component analysis (PCA), it identifies a low-rank subspace (in practice $1/8$ of the hidden dimension) in which activation variances are highest, and keep the coefficients within this subspace in high precision, e.g. 8-bit, while quantizing the rest to 4-bit. Within each subspace, invariant random rotation is applied to further suppress outliers. We show that this is a provably optimal mixed precision quantization scheme that minimizes error. With the Llama families of models, we demonstrate that ResQ outperforms recent uniform and mixed precision PTQ methods on a variety of benchmarks, achieving up to 33% lower perplexity on Wikitext than the next best method *SpinQuant*, and a $2.4\times$ speedup over 16-bit baseline. Code is available at github.com/utkarsh-dmx/project-resq.

1 Introduction

Growing capabilities of large language models (LLMs) come with an increasing computational cost at inference time. LLM inference has two distinct stages: *prefilling*, which processes the input prompt and populates the internal state called KV (key-value) cache, and *generation*, where tokens are generated autoregressively. The prefilling stage is compute-bound, requiring trillions of floating-point operations (FLOPs), whereas the generation stage is memory-bound due to iterative accesses and updates of the KV cache. These high computational costs are further amplified by modern LLMs'

large sizes – some exceeding 400 billion parameters – and the increasingly long context lengths that necessitates large KV caches.

Quantization algorithms are powerful and principled approaches to address the immense computational demands of LLMs at both stages of inference. Quantization of weights reduces parameter storage, lowers memory usage of KV cache during generation, whereas activation quantization decreases the complexity of floating-point operation. However, effective low-precision quantization is difficult due to large outliers in activations, which can be $\sim 20\times$ larger than other values (Dettmers et al., 2022). While post-training methods like KIVI (Liu et al., 2024b) and KVQuant (Hooper et al., 2024) achieve 2-bit KV cache quantization, and techniques like GPTQ (Frantar et al., 2022) and AWQ (Lin et al., 2024c) optimize very low-precision weights, quantizing activations below 8-bit precision remains an open challenge.

Recent LLM activation quantization methods feature two useful strategies: *differential treatment of outliers* retain outlier channels in high precision, leading to mixed-precision quantization (e.g., Dettmers et al. 2022; Zhao et al. 2024; Ashkboos et al. 2023; Figure 1a), whereas *invariant random rotation* suppress outliers, leading to less difficult uniform low-precision quantization (e.g., Ashkboos et al. 2024b; Liu et al. 2024a; Figure 1b). Both reduce quantization error and improve signal-to-quantization-noise ratio (Figure 1d,e) locally; yet a notable model performance gap persists from the 16-bit baseline. For example, SpinQuant (Liu et al., 2024a) at 4-bit, applied to Llama-3-8b (Meta, 2024a), exhibits $\sim 20\%$ higher perplexity than 16-bit baseline, even after extensive optimization.

To mend this gap, we introduce *ResQ*, a novel quantization method that combines the strengths of both aforementioned strategies and thereby improve model efficiency with aggressive 4-bit quanti-

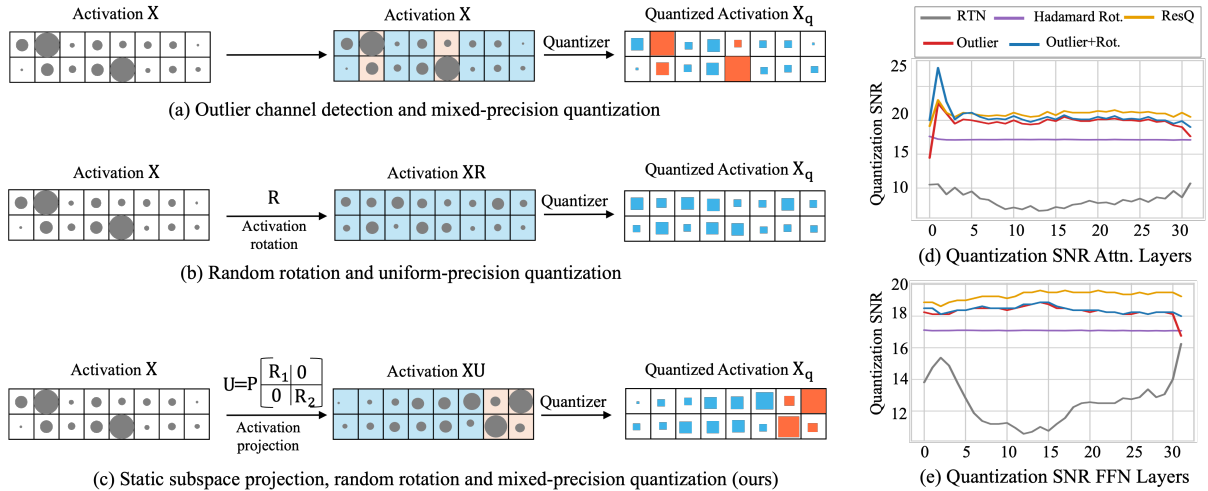


Figure 1: (a)-(c) Different approaches to quantization including ResQ. Symbol sizes represent magnitudes of values and colors indicate precisions of quantization (blue: low precision, orange: high precision). (d)-(e) Quantization SNR comparison of ResQ with other baselines.

zation of activation, weight, and KV cache. Specifically, by means of principal component analysis (PCA), we first identify a low-rank subspace that captures highest variances in activation, and mark the coefficients along this subspace for high-precision (8-bit) and the complement subspace for low-precision (4-bit) quantization. We prove that so doing minimizes quantization error. Moreover, ResQ employs invariant random rotations within each subspace before quantization to further suppress outliers (Figure 1c,d,e). Similar to SpinQuant, most projection matrices can be fused into adjacent weights, leading to minimal runtime computational overhead (Section 4.3). Furthermore, ResQ can be applied to KV cache quantization as well, and can be combined with GPTQ (Frantar et al., 2022), resulting in even better generalizing LLMs.

In practice, one could naïvely combine outlier-based and rotation-based quantization methods. For example, high-precision outliers could be detected using the ℓ_∞ norm similar to QUIK (Ashkboos et al., 2023), and random rotations could be applied within both high- and low-precision quantization groups, as in QuaRot (Ashkboos et al., 2024b). However, such approaches fare less well than ResQ (Figure 1d and 1e) in practice, in support of ResQ’s provably optimal treatment of outlier quantization. When quantizing weight, activation and KV cache to 4-bit with only $1/8$ channels in 8-bit, ResQ achieves 2-33% lower perplexity on Wikitext and 1-5.5% zero-shot accuracy improvements over SpinQuant (Liu et al., 2024a), the best competing method in practice. Unlike SpinQuant,

ResQ does not require gradient-based optimization, making it an easier and faster PTQ solution. Additionally, the rank r of the high-precision subspace can be tuned, giving rise to Pareto-optimal solutions as a tradeoff between computational efficiency and accuracy.

We claim the following contributions.

1. We propose ResQ, a mixed precision weight, activation, and KV cache quantization method by keeping low-rank, high-variance components in high precision, in combination with random rotation-induced outlier suppression.
2. We theoretically analyze the projection matrices in ResQ and show that using PCA-based projections minimizes quantization error.
3. We conduct extensive experiments on various models and language tasks and show that ResQ outperforms related state-of-the-art approaches.
4. We develop hardware kernels and achieve runtime speedup on NVIDIA A100 GPU with our quantized models.

2 Prior Work

2.1 Quantization of LLMs

Quantization reduces model size and accelerates inference by lowering neural network bit precision (Choi et al., 2018; Hubara et al., 2021; Yao et al., 2022; Park et al., 2022; Gholami et al., 2022; Xi et al., 2023). It is broadly categorized into two

categories: *uniform precision quantization* (UPQ) and *mixed precision quantization* (MPQ).

Uniform precision quantization (UPQ) applies the same bit-width across all layers, simplifying implementation but neglecting layer-specific sensitivity to quantization.

Weight-only UPQ methods reduce storage by compressing weights, using techniques like Hessian-guided rounding (GPTQ, Frantar et al. 2022), adaptive rounding (QuIP, Chee et al. 2024), channel-wise scaling (AWQ, Lin et al. 2024c), and multi-codebook quantization (AQLM, Egiazarian et al. 2024). However, these methods struggle with batch processing due to significant activation memory overhead. **Weight-activation UPQ** compresses both weights and activations to address this. Methods such as SmoothQuant (Xiao et al., 2023) and OmniQuant (Shao et al., 2023) scale activations and weights to handle outliers, while RPTQ (Yuan et al., 2023a), QLLM (Liu et al., 2023a), and QServe (Lin et al., 2024d) employ channel-level strategies like clustering and reordering. Rotation-based methods such as QuaRot (Ashkboos et al., 2024b), SpinQuant (Liu et al., 2024a) and DuQuant (Lin et al., 2024b) further enhance robustness in low-precision scenarios. **KV cache UPQ** reduces memory for large batches or long contexts. FlexGen (Sheng et al., 2023) employs 4-bit quantization and memory offloading, while KIVI (Liu et al., 2024b) uses asymmetric 2-bit quantization for compression, enabling efficient inference.

Mixed precision quantization (MPQ) optimizes bit-widths by adapting to the sensitivity of weights and activations, achieving better accuracy than UPQ at similar compression rates. *Our proposed method, ResQ, follows the MPQ approach.*

Weight-only MPQ has advanced efficiency for memory-bound applications with minimal activation demands. Methods like OWQ (Lee et al., 2024) and SpQR (Dettmers et al., 2023) mitigate activation outliers’ impact by retaining critical features in full precision, while SqueezeLLM (Kim et al., 2023) employs Dense-and-Sparse decomposition to efficiently store sensitive weights. **Weight-activation MPQ** enhances efficiency by addressing activation outliers (e.g. Guan et al. 2024; Zeng et al. 2024). Methods like LLM.int8() (Dettmers et al., 2022) and QUIK (Ashkboos et al., 2023) preserve critical activations with mixed or low-precision decompositions, while Atom (Zhao et al., 2024) and SliM-LLM (Huang et al., 2024) optimize quantization through channel reordering and salience-

driven bit allocation. **KV cache MPQ** reduces memory usage while preserving precision for critical tokens using techniques like non-uniform quantization, importance-aware precision, and salient token compression (Hooper et al., 2024; Yang et al., 2024; Dong et al., 2024; He et al., 2024). Alternatively, GEAR quantizes all tokens’ KV cache and maintains quantization error in a low-rank form (Kang et al., 2024).

2.2 Low-rank Decomposition

Low-rank decomposition techniques have been widely used in model compression, reducing dimensionality while maintaining performance. For instance, SliceGPT (Ashkboos et al., 2024a) projects weight matrices onto principal components for sparsification, while ESPACE (Sakr and Khailany, 2024) reduces activation dimensionality via pre-calibrated projections, achieving inference-time efficiency. Similarly, ASVD (Yuan et al., 2023b) introduces an activation-aware decomposition method that incorporates activation distributions into weight decomposition.

Additionally, low-rank decomposition can be applied to reduce KV cache size. For example, Eigen Attention (Saxena et al., 2024) and ASVD (Yuan et al., 2023b) employ low-rank approximations to reduce memory usage in KV caches during attention operations. PALU (Chang et al., 2024) introduces learnable projections to adaptively compress KV caches based on the compression budget. Finally, Matryoshka KV Cache refines this with hierarchical orthogonal projections and knowledge distillation (Lin et al., 2024a).

3 Quantization

Quantization of weight, activation or KV cache involves converting component elements to low precision so that they can be represented using fewer bits for more efficient compute and storage. The N -bit integer quantization and dequantization process on matrix \mathbf{X} is given as

$$Q_N(\mathbf{X}) = \left\lfloor \frac{\mathbf{X} - z_X}{s_X} \right\rfloor \cdot s_X + z_X, \quad (1)$$

where $\lfloor \cdot \rfloor$ is a round-and-clip function; s_X and z_X the scale and zero-point; $z_X = 0$, $s_X = \frac{\max(|\mathbf{X}|)}{2^{N-1}-1}$ for symmetric quantization or $z_X = \min(\mathbf{X})$, $s_X = \frac{\max(\mathbf{X}) - \min(\mathbf{X})}{2^N - 1}$ for asymmetric quantization.

4 ResQ

In this section, we introduce ResQ, a mixed-precision quantization approach that projects weights, activations, and the KV cache into an orthogonal space, retaining the low-rank components in high precision (8-bit) and the rest in low precision. We describe the quantization scheme, the generation of the basis space, provide theoretical guarantees, and outline end-to-end LLM inference deployment procedure.

4.1 Quantization scheme

Given input activation $\mathbf{X} \in \mathbb{R}^{n \times d}$ and weight $\mathbf{W} \in \mathbb{R}^{d \times d}$, they are first projected onto an orthogonal basis defined by the vectors $\mathbf{U} \in \mathbb{R}^{d \times d}$. The coefficients of the projections along this basis are then subject to quantization. We seek to quantize some coefficients along certain bases at high precision while those remaining at low precision. Within \mathbb{R}^d , denote bases of a low-rank space of high-precision components by $\mathbf{U}_h \in \mathbb{R}^{d \times r}$ and those of its complementary subspace of low-precision components by $\mathbf{U}_l \in \mathbb{R}^{d \times (d-r)}$. The rank r controls the amount of components in high precision (in practice we typically choose $r = d/8$). We have $\mathbf{U}_h \mathbf{U}_h^\top + \mathbf{U}_l \mathbf{U}_l^\top = \mathbf{U} \mathbf{U}^\top = \mathbf{I}$ because \mathbf{U} is orthogonal.

The quantized activation \mathbf{X}_q is thusly

$$\mathbf{X}_q = Q_L(\mathbf{X} \mathbf{U}_l) \mathbf{U}_l^\top + Q_H(\mathbf{X} \mathbf{U}_h) \mathbf{U}_h^\top \quad (2)$$

Similarly, quantized weights \mathbf{W}_q is obtained by projecting the inputs space of weights and quantizing the coefficients,

$$\mathbf{W}_q = \mathbf{U}_l Q_L(\mathbf{U}_l^\top \mathbf{W}) + \mathbf{U}_h Q_H(\mathbf{U}_h^\top \mathbf{W}). \quad (3)$$

And the output of the layer is,

$$\begin{aligned} \mathbf{X}_q \mathbf{W}_q &= Q_L(\mathbf{X} \mathbf{U}_l) Q_L(\mathbf{U}_l^\top \mathbf{W}) \\ &\quad + Q_H(\mathbf{X} \mathbf{U}_h) Q_H(\mathbf{U}_h^\top \mathbf{W}). \end{aligned} \quad (4)$$

We make two observations due to orthogonality. First, *the introduction of the projections do not alter the output of the model at infinite precision*. This means that, if quantization operation is removed from Equation 4, the layer output is numerically invariant. Second, *multiplication between low- and high-precision components vanishes (Figure 2)*. This is efficient because only hardware kernels for quantized GEMM between operands of same precision are required.

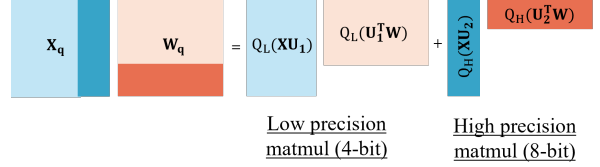


Figure 2: Matrix multiplication with mixed precision operands

4.2 Projections and optimality thereof

The orthogonal basis vectors \mathbf{U} should intuitively have two properties: (1) the low-rank space for high-precision quantization should capture the more important components, and (2) quantization error in both high- and low-precision groups should be minimized. We construct \mathbf{U} as a combination of two rotation matrices serving both objectives respectively. We write $\mathbf{U}_i = \mathbf{P}_i \mathbf{R}_i$, $i \in \{h, l\}$. Therefore,

$$\mathbf{U} = \mathbf{P} \mathbf{R} = [\mathbf{P}_l \ \mathbf{P}_h] \begin{bmatrix} \mathbf{R}_l & \mathbf{0} \\ \mathbf{0} & \mathbf{R}_h \end{bmatrix}, \quad (5)$$

where, $\mathbf{P}_l, \mathbf{R}_l \in \mathbb{R}^{d \times (d-r)}$, $\mathbf{P}_h, \mathbf{R}_h \in \mathbb{R}^{d \times r}$. Inspired by prior work (Ashkboos et al., 2024b; Chee et al., 2024), we make $\mathbf{R}_l, \mathbf{R}_h$ random orthogonal matrices because random rotation reduces outliers, making the rotated matrices easier to quantize. Furthermore, projecting data using a random orthogonal matrix increases Gaussianity of the activations and weights within high- and low-precision groups, due to Lemma 4.1, conducive to the quantizations applied to these groups.

Lemma 4.1. *By Central Limit Theorem, the distribution after multiplication with random orthogonal matrix follows an approximately bell-shaped Gaussian distribution (Chee et al., 2024).*

To determine \mathbf{P} , we minimize the activation quantization error $\|\mathbf{X} - \mathbf{X}_q\|_F$. For activations quantized according to Equation 2, we have,

$$\begin{aligned} \|\mathbf{X} - \mathbf{X}_q\|_F &= \|\mathbf{X} \mathbf{U}_l - Q_L(\mathbf{X} \mathbf{U}_l)\|_F \\ &\quad + \|\mathbf{X} \mathbf{U}_h - Q_H(\mathbf{X} \mathbf{U}_h)\|_F. \end{aligned} \quad (6)$$

Theorem 4.2. *For any matrix \mathbf{X} quantized to \mathbf{X}_q according to method described in Equation 2, assuming the values to be quantized in \mathbf{X} are nor-*

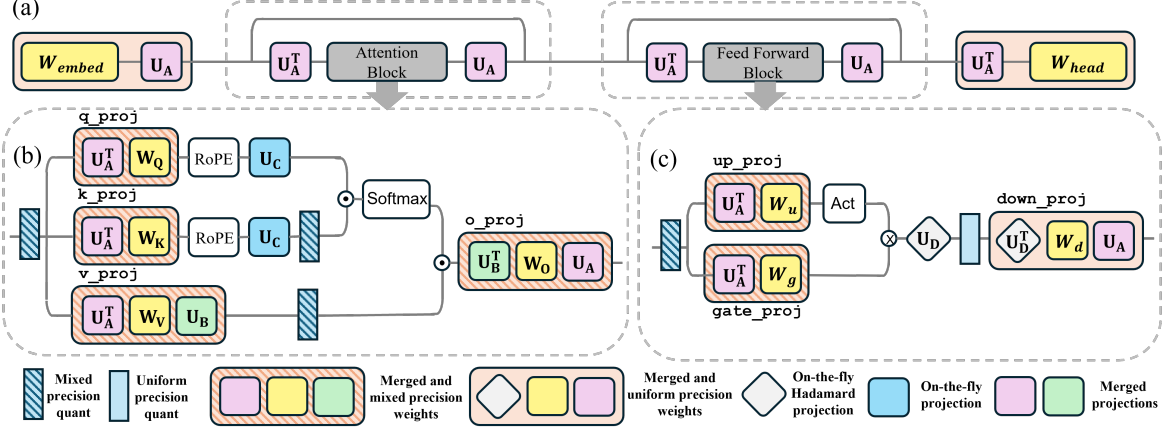


Figure 3: Model inference with ResQ incorporating the projection matrices. (a) U_A modifies the inputs across blocks enabling better quantization. (b) U_B, U_C enables mixed precision quantization of KV cache. (c) U_D projects the activations and weights of down_proj layer.

mally distributed, we have

$$\begin{aligned} \mathbb{E}\|\mathbf{X} - \mathbf{X}_q\|_F &\leq \frac{\sqrt{\pi \log(d-r)}}{2^{L-1} - 1} \mathbb{E}\|\mathbf{X}\|_F \\ &\quad - \left[\frac{\sqrt{\pi \log(d-r)}}{2^{L-1} - 1} - \frac{\sqrt{\pi \log r}}{2^{H-1} - 1} \right] \\ &\quad \mathbb{E}\|\mathbf{X} \mathbf{P}_h\|_F. \end{aligned} \quad (7)$$

Proof of Theorem 4.2 can be found Appendix A.1. Theorem 4.2 bounds the quantization error in Equation 6. To lower the upper bound of quantization error, it is required to maximize $\|\mathbf{X} \mathbf{P}_h\|_F$ which happens when \mathbf{P}_h comprises of eigenvectors of the covariance matrix $\mathbf{X} \mathbf{X}^\top$ with its *largest* eigenvalues. Therefore the low-rank subspace for high-precision quantization can be obtained by means of PCA, while the subspace for low-precision quantization can be obtained using $\mathbf{U}_h \mathbf{U}_h^\top + \mathbf{U}_l \mathbf{U}_l^\top = \mathbf{P}_h \mathbf{P}_h^\top + \mathbf{P}_l \mathbf{P}_l^\top = \mathbf{I}$ (because \mathbf{R}_i is orthogonal). If we construct \mathbf{P} by taking eigenvectors of $\mathbf{X} \mathbf{X}^\top$ arranged in *increasing* order of eigenvalues, the last r columns of such a \mathbf{P} would correspond to \mathbf{P}_h and the first $d-r$ columns would correspond to \mathbf{P}_l . Appendix A.2 shows the distribution of activations after projecting them to the space U .

4.3 Inference computation with optimized projections

Once the projection matrices are obtained, the operation defined in Equation 4 requires multiplying the weights and activations with U . Weights can

be projected and quantized offline. The projection operation on an activation can be merged to the weight of a previous linear layer. Based on the architecture of decoder based LLMs, we introduce four different kinds of projections (Figure 3): $U_A \in \mathbb{R}^{d_h \times d_h}$, $U_B, U_C \in \mathbb{R}^{d_{head} \times d_{head}}$, $U_D \in \mathbb{R}^{d_{FFN} \times d_{FFN}}$ where d_h is hidden dimension of LLM, d_{head} is the attention head dimension and d_{FFN} the hidden dimension of feedforward network.

Projections at block boundaries Input activations to attention and feed forward blocks are projected via U_A . Projection is handled by post multiplying the weight matrix of final linear layer in each block (o_proj in attention and $down_proj$ in feed forward) by U_A . Thus, projections of activations is handled at no additional inference cost. To maintain numerical invariance, the first linear layer of each block ($q|k|v_proj$ in attention and $up_proj|gate_proj$ in feed forward) is pre multiplied by U_A^\top (Figure 3 a). Similarly, the weights of the embedding layer and the final head are modified to manage projection of the residual stream.

Projections within the attention block U_B, U_C ensures that activations within attention block are projected (Figure 3b). Post-multiplication of value projection layer by U_B ensures that value vectors in KV cache are projected and quantized optimally. Consequently, the weights of o_proj layer need to be pre multiplied by U_B^\top to ensure numerical invariance. U_C ensures that the quantization of key in KV cache is handled optimally. To achieve that, it is required to project both the query and key using

Family	Method	Training Free	Llama-2-7b			Llama-2-13b		
			Wiki (↓)	Avg. 0-shot (↑)	MMLU (↑)	Wiki (↓)	Avg. 0-shot (↑)	MMLU (↑)
Llama-2	16-bit	✓	5.5	64.1	41.1	4.9	66.5	52.7
	RTN	✓	1766.2	37.4	23.6	3543.9	33.5	23.6
	GPTQ	✓	9600.0	38.9	23.8	3120.0	33.8	24.8
	SmoothQuant+	✓	15.4	46.1	24.2	11.2	51.0	26.6
	QUIK	✓	7.5	57.0	27.8	6.8	60.2	36.7
	QuaRot	✓	6.1	60.7	32.3	5.4	63.8	47.7
	SpinQuant	✗	6.0	61.0	34.8	5.2	64.8	47.8
ResQ	✓	5.8	62.0	37.7	5.1	65.2	50.1	
Family	Method	Training Free	Llama-3-8b			Llama-3-70b		
			Wiki (↓)	Avg. 0-shot (↑)	MMLU (↑)	Wiki (↓)	Avg. 0-shot (↑)	MMLU (↑)
Llama-3	16-bit	✓	6.1	67.1	63.1	2.9	73.1	75.9
	RTN	✓	218.9	39.3	23.6	452.7	45.5	23.2
	GPTQ	✓	166.3	39.8	23.3	11.6e3	34.9	25.5
	SmoothQuant+	✓	78.2	42.5	24.7	-	-	-
	QUIK	✓	14.2	51.6	32.7	8.0	58.2	51.1
	QuaRot	✓	7.8	62.1	53.2	5.7	67.6	65.3
	SpinQuant	✗	7.4	63.8	56.2	6.2	65.7	59.4
ResQ	✓	7.1	63.9	57.2	4.1	71.1	73.9	
Family	Method	Training Free	Llama-3.2-1b			Llama-3.2-3b		
			Wiki (↓)	Avg. 0-shot (↑)	MMLU (↑)	Wiki (↓)	Avg. 0-shot (↑)	MMLU (↑)
Llama-3.2	16-bit	✓	9.8	54.9	36.9	7.8	62.7	54.8
	RTN	✓	329.1	38.1	23.8	268.8	38.7	25.7
	GPTQ	✓	108.9	38.0	24.9	178.3	40.3	24.8
	SmoothQuant+	✓	228.9	38.0	24.1	96.1	39.0	25.9
	QUIK	✓	21.8	44.3	25.1	15.8	48.8	31.1
	QuaRot	✓	14.3	49.0	25.5	10.1	56.1	42.0
	SpinQuant	✗	13.6	48.8	25.6	9.2	57.9	44.2
ResQ	✓	12.4	50.1	29.4	8.8	59.0	49.8	

Table 1: Comparison of perplexity score on Wikitext, average zero-shot common sense reasoning accuracy and average zero-shot MMLU accuracy at $W/A/KV = 4/4/4$. Results of all techniques were obtained using their official codebase. Our work ResQ and QUIK (Ashkboos et al., 2023) keep $1/8$ th channels in 8-bit. All techniques except RTN use GPTQ (Frantar et al., 2022) for weight quantization. \uparrow higher is better, \downarrow : lower is better. Full results in App. A.3

the same projection matrix U_C . The attention dot product remains invariant under projected inputs,

$$\mathbf{q}_{\text{proj}} \mathbf{K}_{\text{proj}}^\top = (\mathbf{q} U_C)(U_C^\top \mathbf{K}^\top) = \mathbf{q} \mathbf{K}^\top. \quad (8)$$

Where \mathbf{q} and \mathbf{K} are query and key after rotary embedding (RoPE) respectively. Unfortunately, U_C cannot be merged into the previous linear layer due to presence of RoPE and the projection is applied on the fly. To make the on the fly projection efficient, we apply uniform precision quantization to U_C and corresponding input activations.

Projections within the feedforward block U_D ensure improved quantization of activation within feed forward block (Figure 3c). U_D^\top is pre-multiplied with weights of down_proj while due to the presence of activation function within the block, U_D cannot be merged to weights of preceding linear layer and is left on the fly as well. U_D is applied to the hidden dimension of the feed forward network (d_{FFN}) which is 3 to 4 times greater than the hidden dimension of LLM in most language models. In this scenario, matrix multiplication with U_D is extremely expensive in computation and stor-

age. To minimize the overhead, we choose U_D to be a hadamard matrix to leverage fast and efficient hadamard transform kernel. And, we choose weights and activations for down_proj layer to be uniformly quantized to low precision.

5 Experiments

5.1 Setup

Models, tasks, datasets and baselines We conduct experiments on Llama 2 (Touvron et al., 2023), Llama 3 (Meta, 2024a) and very recent Llama 3.2 (Meta, 2024b) models. We benchmark our approach against GPTQ (Frantar et al., 2022), QuaRot (Ashkboos et al., 2024b), QUIK (Ashkboos et al., 2023), SpinQuant (Liu et al., 2024a) and SmoothQuant+, a stronger baseline created by combining SmoothQuant (Xiao et al., 2023) with GPTQ following (Sharify et al., 2024). We evaluate the quantization approaches on a range of tasks which measure the *language modeling ability*: perplexity on Wikitext (Merity et al., 2016), *common sense reasoning ability*: average 0-shot accuracy on Arc-c/e (Clark et al., 2018), BoolQ (Clark et al.,

Model	Method	Training Free	GSM8K 5-shot (\uparrow)		Long Bench (\uparrow)		
			flexible extract	strict match	qmsum	samsun	repobench-p
Llama-3-8b	16-bit	✓	51.0	50.6	23.9	44.8	66.4
	QUIK	✓	2.3	0.0	10.5	25.2	37.6
	QuaRot	✓	27.6	27.1	22.0	43.8	60.6
	SpinQuant	✗	29.8	29.6	23.0	43.9	62.6
	ResQ	✓	33.6	33.2	23.1	44.1	62.3
Llama-3.2-3b	16-bit	✓	25.1	24.9	23.1	43.0	64.4
	QUIK	✓	2.5	0.0	15.9	31.7	30.9
	QuaRot	✓	10.1	9.1	20.6	39.5	56.8
	SpinQuant	✗	11.6	11.4	21.7	41.9	59.1
	ResQ	✓	17.1	16.7	21.7	43.0	61.5

Table 2: Comparison of performance of quantization approaches on generative tasks at precisions of $W/A/KV = 4/4/4$ bits. Our work ResQ and QUIK (Ashkboos et al., 2023) keep $1/8$ th of channels in 8-bit.

2019), HellaSwag (Zellers et al., 2019), Openbook QA (Mihaylov et al., 2018), PIQA (Bisk et al., 2020), SIQA (Sap et al., 2019), WinoGrande (Sakaguchi et al., 2021), *language understanding*: 0-shot accuracy on MMLU (Hendrycks et al., 2021), *mathematical understanding*: 5-shot GSM8K (Cobbe et al., 2021), *dialogue summarization*: samsun (Gliwa et al., 2019) and qmsun (Zhong et al., 2021) from LongBench (Bai et al., 2024), and *code completion*: repobench-p (Liu et al., 2023b) from LongBench.

Implementation details We implement ResQ using the HuggingFace Transformers library (Wolf et al., 2020) with PyTorch (Paszke et al., 2019). We share a single U_A across all layers, while U_B , U_C and U_D are generated per layer. Following SpinQuant (Liu et al., 2024a), we use per-token asymmetric quantization for activations, per-channel symmetric quantization for weights, and per-head asymmetric quantization for the KV cache. We fuse the projection matrices U_A , U_B , U_D into weights and apply GPTQ (Frantar et al., 2022) for weight quantization. To efficiently implement on-the-fly projections, U_D is a Hadamard matrix and U_C and its corresponding activations are quantized to 8-bit. The entire process, including obtaining projections and quantization, runs on a single NVIDIA A100 GPU; for Llama-3-8B, it takes 35 minutes. Additional details are in Appendix A.4.

5.2 Main Results

Language modeling, understanding, and reasoning tasks We evaluate ResQ on tasks that test language modelling ability (Perplexity on Wikitext), common sense reasoning ability (average 0-shot accuracy on the eight tasks listed in section 5.1) and language understanding (average 0-shot accuracy on MMLU). The results are presented in Table 1. We see that ResQ reduces the gap to 16-

W/A/KV	Method	Llama-3-8b	Llama-3.2-3b
4/4/4	outlier+rot	7.2	9.0
	ResQ	7.1	8.8
4/8/4	outlier+rot	6.6	8.3
	ResQ	6.5	8.2
3/8/3	outlier+rot	7.7	9.9
	ResQ	7.5	9.8
2/8/8	outlier+rot	12.6	16.0
	ResQ	12.1	15.7
3/3/3	outlier+rot	14.7	18.7
	ResQ	14.6	17.5

Table 3: Wikitext perplexity comparison of ResQ and baseline which keeps channels with high l_∞ norm in high precision and uses rotation to reduce quantization error within high precision and low precision groups.

bit performance and outperforms the quantization baselines across all tasks on all models. Particularly, ResQ outperforms SpinQuant by achieving 2-33% lower Wikitext perplexity, 0.3-5.4% better average zero-shot accuracy and a 1-14.5% better accuracy on MMLU benchmark across the models tested without any additional training. Compared with QUIK, another mixed precision quantization approach, ResQ achieves 22-50% better perplexity, 5-12.3% better average zero shot accuracy and 4.3-24.5% better MMLU accuracy over all models.

Generative tasks We also test ResQ on tasks that require auto-regressive token generation including the GSM8K mathematical understanding benchmark, dialogue summarization benchmarks (qmsun and samsun) and code completion benchmark (repobench-p) (in Table 2). The goal of choosing these tasks is to evaluate the generation ability on a wide variety of domains. On the challenging GSM8K benchmark where QUIK fails to produce meaningful results, ResQ outperforms SpinQuant by 3.8% and 5.5% on the 8b and 3b parameter model respectively, closing the gap to 16-bit baseline. On Long Bench evaluation tasks, ResQ

	ResQ	Removed Projections				
		U_D	U_A	U_B	U_C	U_C, U_B
Llama-2-7b	5.8	1550	2500	5.8	5.9	5.9
Llama-3-8b	7.1	1607	37.4	7.2	7.3	7.4
Llama-3.2-3b	8.8	279.2	39.0	9.0	9.2	9.4

Table 4: Impact of different projections in ResQ. Evaluated by removing individual components and observing Wikitext perplexity.

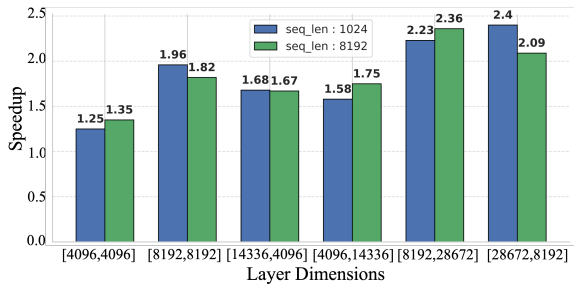


Figure 4: Layerwise speedup with ResQ on NVIDIA A100 over 16-bit baseline

demonstrates competitive performance and outperforms SpinQuant without any additional training.

Comparison against outliers with rotation baseline A stronger baseline can be created combining existing quantization approaches. Like QUIK, one can find channels which consistently contain outliers and keep them in 8-bit while keep the remaining channels in low precision. And, the quantization of high/low precision groups can be improved using random rotations introduced in QuaRot. Compared with such a baseline which keeps channels with high l_∞ norm in 8-bit, ResQ’s unique approach involves keeping coefficients along basis vectors with high eigenvalues in 8-bit. We see in Table 3 that ResQ consistently outperforms such a strong baseline across various precisions of W/A/KV highlighting ResQ’s PCA driven theoretically optimal approach of choosing high precision components.

5.3 Hardware performance

We implement the mixed-precision quantization using CUDA 11.8 and PyTorch. We use CUTLASS (Thakkar et al., 2023) to perform int4 and int8 GEMM operations on TensorCore. We achieve about $1.25\times$ to $2.4\times$ speedup with ResQ over 16-bit baseline tested across several layer dimensions found in Llama models tested on NVIDIA A100 GPUs (Figure 4). We observe that larger layers achieve higher speedup with ResQ.

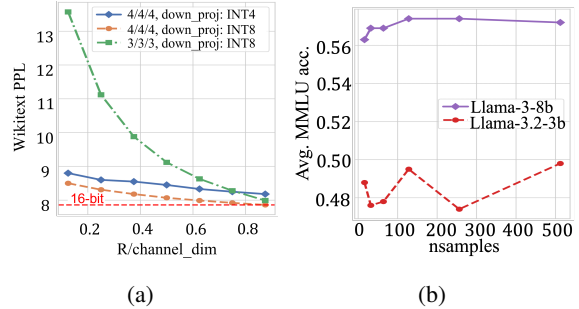


Figure 5: Ablation study on (a) Changing rank of high precision subspace for Llama-3.2-3b and (b) Changing number of calibration samples.

5.4 Ablation studies

Projection bases We evaluate the impact of different projections employed in ResQ by removing them and evaluating performance in Table 4. We see that removing U_D or U_A has a catastrophic impact on perplexity highlighting the importance of the projections. U_B and U_C which aid in quantization of KV cache have less severe impact when removed independently. But removing both of them leads to a non trivial increase in perplexity (particularly for Llama-3-8b and Llama-3.2-3b which employ grouped query attention).

Rank of high-precision subspace ResQ allows for seamless trade-off between accuracy and performance by modulating the rank r of high precision subspace (Figure 5a). Increasing the rank improves perplexity albeit at the cost of increased computations in high precision.

Calibration dataset We change number of Wikitext calibration samples used to obtain projections and evaluate performance in Figure 5b. We see that for Llama-3-8b, MMLU accuracy increases with increasing samples and saturates beyond 128 samples. For Llama-3.2-3b, the trend is unclear with 512 samples achieving best performance.

6 Conclusion

We introduce ResQ, a novel mixed-precision PTQ technique toward 4-bit quantization of large language models. ResQ projects weight, activation, and KV cache tensors to subspaces spanned by principal components, quantizing a low-rank ($1/8$ of hidden dimension) high-variance subspace to 8-bit and the rest to 4-bit. ResQ achieves superior performance to both uniform- and mixed-precision quantization methods. We demonstrate the effectiveness of ResQ across a variety of tasks—including language modeling, language understanding, common-

sense reasoning, and language generation—using the Llama families of models. Compared to SpinQuant, the most competitive baseline, ResQ achieves up to 33% lower perplexity on the Wiki-Text dataset without requiring any additional training and offers up to $2.4\times$ speedup over the 16-bit baseline.

Limitations

ResQ takes a significant step towards efficiently serving LLMs in resource-constrained, on-device scenarios, potentially expanding the application space for these models. While we demonstrate our approach using the Wikitext (Merity et al., 2016) dataset, we have not yet extensively explored whether other datasets might yield projection matrices that better optimize performance on downstream tasks. Additionally, we maintain a constant rank r for the high-precision subspace across all layers, which may not be optimal. Identifying the ideal rank for each layer to balance accuracy and efficiency remains a promising direction for future work. Moreover, further optimization of projection matrices using a training based approach proposed in SpinQuant (Liu et al., 2024a) would extend the improvements with our approach. But the resource intensive nature of such an approach has prohibited us from exploring the potential direction. Finally, although our approach aims to make LLMs more accessible and widespread, it does not address the potential risks of misuse for malicious purposes. To mitigate these risks, a strong commitment to user data protection, clear ethical guidelines, and transparency mechanisms is essential.

Acknowledgment

The authors would like to thank Wanzin Yazar and Tristan Webb for infrastructure and technical assistance and Zifei Xu for helpful discussions. This work was supported by the Center for the Co-Design of Cognitive Systems (COCOSYS), a DARPA sponsored JUMP center of Semiconductor Research Corporation (SRC), Intel, SRC AIHW Program.

References

Saleh Ashkboos, Maximilian L Croci, Marcelo Genari do Nascimento, Torsten Hoefler, and James Hensman. 2024a. SliceGPT: Compress large language models by deleting rows and columns. *arXiv preprint arXiv:2401.15024*.

Saleh Ashkboos, Iliia Markov, Elias Frantar, Tingxuan Zhong, Xincheng Wang, Jie Ren, Torsten Hoefler, and Dan Alistarh. 2023. QUIK: Towards end-to-end 4-bit inference on generative large language models. *arXiv:2310.09259*.

Saleh Ashkboos, Amirkeivan Mohtashami, Maximilian L Croci, Bo Li, Pashmina Cameron, Martin Jaggi, Dan Alistarh, Torsten Hoefler, and James Hensman. 2024b. QuaRot: Outlier-free 4-bit inference in rotated llms. *arXiv:2404.00456*.

Yushi Bai, Xin Lv, Jiajie Zhang, Hongchang Lyu, Jiankai Tang, Zhidian Huang, Zhengxiao Du, Xiao Liu, Aohan Zeng, Lei Hou, Yuxiao Dong, Jie Tang, and Juanzi Li. 2024. LongBench: A bilingual, multi-task benchmark for long context understanding. In *Proceedings of the 62nd Annual Meeting of the Association for Computational Linguistics (Volume 1: Long Papers)*, pages 3119–3137, Bangkok, Thailand. Association for Computational Linguistics.

Yonatan Bisk, Rowan Zellers, Jianfeng Gao, Yejin Choi, et al. 2020. PIQA: Reasoning about physical commonsense in natural language. In *Proceedings of the AAAI conference on artificial intelligence*, volume 34, pages 7432–7439.

Chi-Chih Chang, Wei-Cheng Lin, Chien-Yu Lin, Chong-Yan Chen, Yu-Fang Hu, Pei-Shuo Wang, Ning-Chi Huang, Luis Ceze, Mohamed S Abdelfattah, and Kai-Chiang Wu. 2024. Palu: Compressing kv-cache with low-rank projection. *arXiv preprint arXiv:2407.21118*.

Jerry Chee, Yaohui Cai, Volodymyr Kuleshov, and Christopher M De Sa. 2024. QuIP: 2-bit quantization of large language models with guarantees. *Advances in Neural Information Processing Systems*, 36.

Jungwook Choi, Zhuo Wang, Swagath Venkataramani, Pierce I-Jen Chuang, Vijayalakshmi Srinivasan, and Kailash Gopalakrishnan. 2018. PACT: Parameterized clipping activation for quantized neural networks. *arXiv:1805.06085*.

Christopher Clark, Kenton Lee, Ming-Wei Chang, Tom Kwiatkowski, Michael Collins, and Kristina Toutanova. 2019. Boolq: Exploring the surprising difficulty of natural yes/no questions. *Preprint*, arXiv:1905.10044.

Peter Clark, Isaac Cowhey, Oren Etzioni, Tushar Khot, Ashish Sabharwal, Carissa Schoenick, and Oyvind Tafjord. 2018. Think you have solved question answering? try arc, the ai2 reasoning challenge. *arXiv preprint arXiv:1803.05457*.

Karl Cobbe, Vineet Kosaraju, Mohammad Bavarian, Jacob Hilton, Reiichiro Nakano, Christopher Hesse, and John Schulman. 2021. Training verifiers to solve math word problems. *Preprint*, arXiv:2110.14168.

Tim Dettmers, Mike Lewis, Younes Belkada, and Luke Zettlemoyer. 2022. Gpt3. int8 (): 8-bit matrix multiplication for transformers at scale. *Advances in*

- Neural Information Processing Systems*, 35:30318–30332.
- Tim Dettmers, Ruslan Svirschevski, Vage Egiazarian, Denis Kuznedelev, Elias Frantar, Saleh Ashkboos, Alexander Borzunov, Torsten Hoefler, and Dan Alistarh. 2023. SpQR: A sparse-quantized representation for near-lossless llm weight compression. *arXiv:2306.03078*.
- Shichen Dong, Wen Cheng, Jiayu Qin, and Wei Wang. 2024. QAQ: Quality adaptive quantization for llm kv cache. *arXiv:2403.04643*.
- Vage Egiazarian, Andrei Panferov, Denis Kuznedelev, Elias Frantar, Artem Babenko, and Dan Alistarh. 2024. Extreme compression of large language models via additive quantization. *arXiv:2401.06118*.
- Elias Frantar, Saleh Ashkboos, Torsten Hoefler, and Dan Alistarh. 2022. GPTQ: Accurate post-training quantization for generative pre-trained transformers. *arXiv:2210.17323*.
- Leo Gao, Jonathan Tow, Baber Abbasi, Stella Biderman, Sid Black, Anthony DiPofi, Charles Foster, Laurence Golding, Jeffrey Hsu, Alain Le Noac’h, Haonan Li, Kyle McDonell, Niklas Muennighoff, Chris Ociepa, Jason Phang, Laria Reynolds, Hailey Schoelkopf, Aviya Skowron, Lintang Sutawika, Eric Tang, Anish Thite, Ben Wang, Kevin Wang, and Andy Zou. 2024. [A framework for few-shot language model evaluation](#).
- Amir Gholami, Sehoon Kim, Zhen Dong, Zhewei Yao, Michael W Mahoney, and Kurt Keutzer. 2022. A survey of quantization methods for efficient neural network inference. In *Low-Power Computer Vision*, pages 291–326. Chapman and Hall/CRC.
- Bogdan Gliwa, Iwona Mochol, Maciej Biesek, and Aleksander Wawer. 2019. Samsun corpus: A human-annotated dialogue dataset for abstractive summarization. *arXiv preprint arXiv:1911.12237*.
- Ziyi Guan, Hantao Huang, Yupeng Su, Hong Huang, Ngai Wong, and Hao Yu. 2024. APTQ: Attention-aware post-training mixed-precision quantization for large language models. In *Proceedings of the 61st ACM/IEEE Design Automation Conference*, pages 1–6.
- Yefei He, Luoming Zhang, Weijia Wu, Jing Liu, Hong Zhou, and Bohan Zhuang. 2024. ZipCache: Accurate and efficient kv cache quantization with salient token identification. *arXiv:2405.14256*.
- Dan Hendrycks, Collin Burns, Steven Basart, Andy Zou, Mantas Mazeika, Dawn Song, and Jacob Steinhardt. 2021. Measuring massive multitask language understanding. *Proceedings of the International Conference on Learning Representations (ICLR)*.
- Coleman Hooper, Sehoon Kim, Hiva Mohammadzadeh, Michael W Mahoney, Yakun Sophia Shao, Kurt Keutzer, and Amir Gholami. 2024. KVQuant: Towards 10 million context length llm inference with kv cache quantization. *arXiv:2401.18079*.
- Wei Huang, Haotong Qin, Yangdong Liu, Yawei Li, Xi-anlong Liu, Luca Benini, Michele Magno, and Xiaojuan Qi. 2024. SliM-LLM: Saliency-driven mixed-precision quantization for large language models. *arXiv:2405.14917*.
- Itay Hubara, Yury Nahshan, Yair Hanani, Ron Banner, and Daniel Soudry. 2021. Accurate post training quantization with small calibration sets. In *International Conference on Machine Learning*, pages 4466–4475.
- Hao Kang, Qingru Zhang, Souvik Kundu, Geonhwa Jeong, Zaoxing Liu, Tushar Krishna, and Tuo Zhao. 2024. Gear: An efficient kv cache compression recipe for near-lossless generative inference of llm. *arXiv preprint arXiv:2403.05527*.
- Sehoon Kim, Coleman Hooper, Amir Gholami, Zhen Dong, Xiuyu Li, Sheng Shen, Michael W Mahoney, and Kurt Keutzer. 2023. SqueezeLLM: Dense-and-sparse quantization. *arXiv:2306.07629*.
- Changhun Lee, Jungyu Jin, Taesu Kim, Hyungjun Kim, and Eunhyeok Park. 2024. OWQ: Outlier-aware weight quantization for efficient fine-tuning and inference of large language models. In *Proceedings of the AAAI Conference on Artificial Intelligence*, volume 38, pages 13355–13364.
- Muyang Li, Yujun Lin, Zhekai Zhang, Tianle Cai, Xiuyu Li, Junxian Guo, Enze Xie, Chenlin Meng, Jun-Yan Zhu, and Song Han. 2024. [Svdquant: Absorbing outliers by low-rank components for 4-bit diffusion models](#). *Preprint*, arXiv:2411.05007.
- Bokai Lin, Zihao Zeng, Zipeng Xiao, Siqi Kou, Tianqi Hou, Xiaofeng Gao, Hao Zhang, and Zhijie Deng. 2024a. Matryoshkav: Adaptive kv compression via trainable orthogonal projection. *arXiv preprint arXiv:2410.14731*.
- Haokun Lin, Haobo Xu, Yichen Wu, Jingzhi Cui, Yingtao Zhang, Linzhan Mou, Linqi Song, Zhenan Sun, and Ying Wei. 2024b. Duquant: Distributing outliers via dual transformation makes stronger quantized llms. In *The Thirty-eighth Annual Conference on Neural Information Processing Systems*.
- Ji Lin, Jiaming Tang, Haotian Tang, Shang Yang, Weiming Chen, Wei-Chen Wang, Guangxuan Xiao, Xingyu Dang, Chuang Gan, and Song Han. 2024c. AWQ: Activation-aware weight quantization for on-device llm compression and acceleration. *Proceedings of Machine Learning and Systems*, 6:87–100.
- Yujun Lin, Haotian Tang, Shang Yang, Zhekai Zhang, Guangxuan Xiao, Chuang Gan, and Song Han. 2024d. QServe: W4a8kv4 quantization and system co-design for efficient llm serving. *arXiv:2405.04532*.

- Jing Liu, Ruihao Gong, Xiuying Wei, Zhiwei Dong, Jianfei Cai, and Bohan Zhuang. 2023a. QLLM: Accurate and efficient low-bitwidth quantization for large language models. *arXiv:2310.08041*.
- Tianyang Liu, Canwen Xu, and Julian McAuley. 2023b. [Repobench: Benchmarking repository-level code auto-completion systems](#). *Preprint*, arXiv:2306.03091.
- Zechun Liu, Changsheng Zhao, Igor Fedorov, Bilge Soran, Dhruv Choudhary, Raghuraman Krishnamoorthi, Vikas Chandra, Yuandong Tian, and Tijmen Blankevoort. 2024a. SpinQuant: Llm quantization with learned rotations. *arXiv:2405.16406*.
- Zirui Liu, Jiayi Yuan, Hongye Jin, Shaochen Zhong, Zhaozhuo Xu, Vladimir Braverman, Beidi Chen, and Xia Hu. 2024b. KIVI: A tuning-free asymmetric 2bit quantization for kv cache. *arXiv:2402.02750*.
- Stephen Merity, Caiming Xiong, James Bradbury, and Richard Socher. 2016. Pointer sentinel mixture models. *arXiv preprint arXiv:1609.07843*.
- Meta. 2024a. [Introducing Meta Llama 3: The most capable openly available LLM to date](#).
- Meta. 2024b. [Llama 3.2: Revolutionizing edge AI and vision with open, customizable models](#).
- Todor Mihaylov, Peter Clark, Tushar Khot, and Ashish Sabharwal. 2018. Can a suit of armor conduct electricity? a new dataset for open book question answering. In *EMNLP*.
- Gunho Park, Baeseong Park, Se Jung Kwon, Byeongwook Kim, Youngjoo Lee, and Dongsoo Lee. 2022. nuqmm: Quantized matmul for efficient inference of large-scale generative language models. *arXiv:2206.09557*.
- Adam Paszke, Sam Gross, Francisco Massa, Adam Lerer, James Bradbury, Gregory Chanan, Trevor Killeen, Zeming Lin, Natalia Gimelshein, Luca Antiga, et al. 2019. Pytorch: An imperative style, high-performance deep learning library. *Advances in neural information processing systems*, 32.
- Keisuke Sakaguchi, Ronan Le Bras, Chandra Bhagavatula, and Yejin Choi. 2021. WinoGrande: An adversarial winograd schema challenge at scale. *Communications of the ACM*, 64(9):99–106.
- Charbel Sakr and Brucek Khailany. 2024. ESPACE: Dimensionality reduction of activations for model compression. *arXiv preprint arXiv:2410.05437*.
- Maarten Sap, Hannah Rashkin, Derek Chen, Ronan Le Bras, and Yejin Choi. 2019. Social iqa: Commonsense reasoning about social interactions. In *Proceedings of the 2019 Conference on Empirical Methods in Natural Language Processing and the 9th International Joint Conference on Natural Language Processing (EMNLP-IJCNLP)*, pages 4463–4473.
- Utkarsh Saxena, Gobinda Saha, Sakshi Choudhary, and Kaushik Roy. 2024. [Eigen attention: Attention in low-rank space for KV cache compression](#). In *Findings of the Association for Computational Linguistics: EMNLP 2024*, pages 15332–15344, Miami, Florida, USA. Association for Computational Linguistics.
- Wenqi Shao, Mengzhao Chen, Zhaoyang Zhang, Peng Xu, Lirui Zhao, Zhiqian Li, Kaipeng Zhang, Peng Gao, Yu Qiao, and Ping Luo. 2023. OmniQuant: Omnidirectionally calibrated quantization for large language models. *arXiv:2308.13137*.
- Sayeh Sharify, Utkarsh Saxena, Zifei Xu, Wanzin Yazar, Ilya Soloveychik, and Xin Wang. 2024. [Post training quantization of large language models with microscaling formats](#). *Preprint*, arXiv:2405.07135.
- Ying Sheng, Lianmin Zheng, Binhang Yuan, Zhuohan Li, Max Ryabinin, Beidi Chen, Percy Liang, Christopher Ré, Ion Stoica, and Ce Zhang. 2023. FlexGen: High-throughput generative inference of large language models with a single gpu. In *International Conference on Machine Learning*, pages 31094–31116. PMLR.
- Vijay Thakkar, Pradeep Ramani, Cris Cecka, Aniket Shivam, Honghao Lu, Ethan Yan, Jack Kosaian, Mark Hoemmen, Haicheng Wu, Andrew Kerr, Matt Nicely, Duane Merrill, Dustyn Blasig, Fengqi Qiao, Piotr Majcher, Paul Springer, Markus Hohnerbach, Jin Wang, and Manish Gupta. 2023. [CUTLASS](#).
- Hugo Touvron, Louis Martin, Kevin Stone, Peter Albert, Amjad Almahairi, Yasmine Babaei, Nikolay Bashlykov, Soumya Batra, Prajjwal Bhargava, Shrubti Bhosale, Dan Bikel, Lukas Blecher, Cristian Canton Ferrer, Moya Chen, Guillem Cucurull, David Esiobu, Jude Fernandes, Jeremy Fu, Wenyin Fu, Brian Fuller, Cynthia Gao, Vedanuj Goswami, Naman Goyal, Anthony Hartshorn, Saghar Hosseini, Rui Hou, Hakan Inan, Marcin Kardas, Viktor Kerkez, Madian Khabsa, Isabel Kloumann, Artem Korenev, Punit Singh Koura, Marie-Anne Lachaux, Thibaut Lavril, Jenya Lee, Diana Liskovich, Yinghai Lu, Yuning Mao, Xavier Martinet, Todor Mihaylov, Pushkar Mishra, Igor Molybog, Yixin Nie, Andrew Poulton, Jeremy Reizenstein, Rashi Rungta, Kalyan Saladi, Alan Schelten, Ruan Silva, Eric Michael Smith, Ranjan Subramanian, Xiaoqing Ellen Tan, Binh Tang, Ross Taylor, Adina Williams, Jian Xiang Kuan, Puxin Xu, Zheng Yan, Iliyan Zarov, Yuchen Zhang, Angela Fan, Melanie Kambadur, Sharan Narang, Aurelien Rodriguez, Robert Stojnic, Sergey Edunov, and Thomas Scialom. 2023. [Llama 2: Open foundation and fine-tuned chat models](#). *Preprint*, arXiv:2307.09288.
- Thomas Wolf, Lysandre Debut, Victor Sanh, Julien Chaumond, Clement Delangue, Anthony Moi, Pierric Cistac, Tim Rault, Rémi Louf, Morgan Funtowicz, Joe Davison, Sam Shleifer, Patrick von Platen, Clara Ma, Yacine Jernite, Julien Plu, Canwen Xu, Teven Le Scao, Sylvain Gugger, Mariama Drame, Quentin Lhoest, and Alexander M. Rush. 2020. [Huggingface’s transformers: State-of-the-art natural language processing](#). *Preprint*, arXiv:1910.03771.

Haocheng Xi, Changhao Li, Jianfei Chen, and Jun Zhu. 2023. Training transformers with 4-bit integers. *Advances in Neural Information Processing Systems*, 36:49146–49168.

Guangxuan Xiao, Ji Lin, Mickael Seznec, Hao Wu, Julien Demouth, and Song Han. 2023. Smoothquant: Accurate and efficient post-training quantization for large language models. In *International Conference on Machine Learning*, pages 38087–38099. PMLR.

June Yong Yang, Byeongwook Kim, Jeongin Bae, Beomseok Kwon, Gunho Park, Eunho Yang, Se Jung Kwon, and Dongsoo Lee. 2024. No Token Left Behind: Reliable kv cache compression via importance-aware mixed precision quantization. *arXiv:2402.18096*.

Zhewei Yao, Reza Yazdani Aminabadi, Minjia Zhang, Xiaoxia Wu, Conglong Li, and Yuxiong He. 2022. ZeroQuant: Efficient and affordable post-training quantization for large-scale transformers. *Advances in Neural Information Processing Systems*, 35:27168–27183.

Zhihang Yuan, Lin Niu, Jiawei Liu, Wenyu Liu, Xinggang Wang, Yuzhang Shang, Guangyu Sun, Qiang Wu, Jiaxiang Wu, and Bingzhe Wu. 2023a. RPTQ: Reorder-based post-training quantization for large language models. *arXiv:2304.01089*.

Zhihang Yuan, Yuzhang Shang, Yue Song, Qiang Wu, Yan Yan, and Guangyu Sun. 2023b. ASVD: Activation-aware singular value decomposition for compressing large language models. *arXiv preprint arXiv:2312.05821*.

Rowan Zellers, Ari Holtzman, Yonatan Bisk, Ali Farhadi, and Yejin Choi. 2019. HellaSwag: Can a machine really finish your sentence? *arXiv preprint arXiv:1905.07830*.

Chao Zeng, Songwei Liu, Yusheng Xie, Hong Liu, Xiaojian Wang, Miao Wei, Shu Yang, Fangmin Chen, and Xing Mei. 2024. ABQ-LLM: Arbitrary-bit quantized inference acceleration for large language models. *arXiv:2408.08554*.

Yilong Zhao, Chien-Yu Lin, Kan Zhu, Zihao Ye, Lequn Chen, Size Zheng, Luis Ceze, Arvind Krishnamurthy, Tianqi Chen, and Baris Kasikci. 2024. Atom: Low-bit quantization for efficient and accurate llm serving. *Proceedings of Machine Learning and Systems*, 6:196–209.

Ming Zhong, Da Yin, Tao Yu, Ahmad Zaidi, Mutethia Mutuma, Rahul Jha, Ahmed Hassan, Asli Celikyilmaz, Yang Liu, Xipeng Qiu, et al. 2021. Qmsum: A new benchmark for query-based multi-domain meeting summarization. In *Proceedings of the 2021 Conference of the North American Chapter of the Association for Computational Linguistics: Human Language Technologies*, pages 5905–5921.

A Appendix

A.1 Proof of Theorem 4.2

We begin the proof by introducing the following lemma.

Lemma A.1. *For any tensor \mathbf{R} quantized following the quantization described in equation 1, assuming the values of \mathbf{R} follows a normal distribution, we have*

$$\mathbb{E}\|\mathbf{R} - Q(\mathbf{R})\|_F \leq \frac{\sqrt{\pi \log[\text{size}(\mathbf{R})]}}{2^{n-1} - 1} \mathbb{E}\|\mathbf{R}\|_F \quad (9)$$

where $\text{size}(\mathbf{R})$ denotes the number of elements in \mathbf{R} .

Proof of lemma A.1 can be found in (Li et al., 2024). From this lemma we obtain that the quantization error $\|\mathbf{R} - Q(\mathbf{R})\|_F$ is bounded by the magnitude of the tensor quantized $\|\mathbf{R}\|_F$. Now for our use case of mixed precision quantization where the low-precision component is quantized to L bits and high precision component is quantized to H bits, we write the quantization error again below,

$$\begin{aligned} \mathbb{E}\|\mathbf{X} - \mathbf{X}_q\|_F &= \mathbb{E}\|\mathbf{X}\mathbf{U}_l - Q_L(\mathbf{X}\mathbf{U}_l)\|_F \\ &\quad + \mathbb{E}\|\mathbf{X}\mathbf{U}_h - Q_H(\mathbf{X}\mathbf{U}_h)\|_F. \end{aligned} \quad (10)$$

The random rotation matrices \mathbf{R} ensure that $\mathbf{X}\mathbf{U}_l$ and $\mathbf{X}\mathbf{U}_h$ are normally distributed by Lemma 4.1. Applying Lemma A.1 to the quantization error in equation 10, we get,

$$\begin{aligned} \|\mathbf{X} - \mathbf{X}_q\|_F &\leq \frac{\sqrt{\log(\text{size}(\mathbf{X}\mathbf{U}_l))\pi}}{2^{L-1} - 1} \mathbb{E}\|\mathbf{X}\mathbf{U}_l\|_F \\ &\quad + \frac{\sqrt{\log(\text{size}(\mathbf{X}\mathbf{U}_h))\pi}}{2^{H-1} - 1} \mathbb{E}\|\mathbf{X}\mathbf{U}_h\|_F \\ &= \frac{\sqrt{\log(\text{size}(\mathbf{X}\mathbf{P}_l))\pi}}{2^{L-1} - 1} \mathbb{E}\|\mathbf{X}\mathbf{P}_l\|_F \\ &\quad + \frac{\sqrt{\log(\text{size}(\mathbf{X}\mathbf{P}_h))\pi}}{2^{H-1} - 1} \mathbb{E}\|\mathbf{X}\mathbf{P}_h\|_F \\ &= \frac{\sqrt{\log(\text{size}(\mathbf{X}\mathbf{P}_l))\pi}}{2^{L-1} - 1} \mathbb{E}\|\text{tr}(\mathbf{X}\mathbf{P}_l\mathbf{P}_l^\top \mathbf{X}^\top)\|_F \\ &\quad + \frac{\sqrt{\log(\text{size}(\mathbf{X}\mathbf{P}_h))\pi}}{2^{H-1} - 1} \mathbb{E}\|\text{tr}(\mathbf{X}\mathbf{P}_h\mathbf{P}_h^\top \mathbf{X}^\top)\|_F \end{aligned} \quad (11)$$

We know $\text{size}(\mathbf{X}\mathbf{P}_l) = d - r$ and $\text{size}(\mathbf{X}\mathbf{P}_h) = r$ since r components are in high precision. With

		Llama-2 family													
Model	Method	0-shot common sense reasoning tasks								0-shot MMLU tasks					
		ARC-c	ARC-e	BoolQ	HellaS	OBQA	PIQA	SIQA	WinoG	Avg.	humanities	Other	SocialS	STEM	Avg.
		(\uparrow)	(\uparrow)	(\uparrow)	(\uparrow)	(\uparrow)	(\uparrow)	(\uparrow)	(\uparrow)	(\uparrow)	(\uparrow)	(\uparrow)	(\uparrow)	(\uparrow)	(\uparrow)
Llama-2-7b	16-bit	46.3	74.6	77.8	75.9	44.2	79.2	46.1	69.1	64.1	38.9	45.9	46.0	33.4	41.1
	RTN	26.3	27.8	54.8	29.4	25.8	51.0	35.0	48.7	37.4	24.5	24.7	22.9	22.2	23.6
	GPTQ	24.8	31.4	55.4	30.6	25.6	55.8	34.2	53.3	38.9	24.7	24.5	22.7	23.2	23.8
	SmoothQuant+	29.3	47.1	56.8	48.6	31.8	65.5	37.2	52.4	46.1	25.0	24.5	24.1	23.4	24.2
	QUIK	39.8	63.7	68.9	68.3	37.8	72.9	42.1	62.4	57.0	26.9	29.6	28.8	25.8	27.8
	QuaRot	41.5	71.4	73.2	73.2	40.6	76.9	43.6	65.6	60.7	31.2	35.1	34.6	28.2	32.3
	SpinQuant	43.6	71.3	73.8	73.2	40.4	76.0	44.1	65.4	61.0	33.9	38.5	37.5	29.5	34.8
	ResQ	44.0	72.6	75.3	74.0	41.0	77.9	43.9	66.9	62.0	35.9	40.9	42.2	32.2	37.7
Llama-2-13b	16-bit	49.1	77.4	80.5	79.4	45.2	80.7	47.2	72.1	66.5	47.9	59.3	61.0	42.4	52.7
	RTN	22.8	29.8	40.2	26.6	27.8	51.4	35.6	50.6	33.5	23.7	25.0	23.1	22.6	23.6
	GPTQ	23.6	31.1	38.7	27.2	26.8	53.6	35.8	49.8	33.8	25.0	25.4	23.7	25.1	24.8
	SmoothQuant+	34.5	55.6	62.9	62.5	32.4	70.1	38.7	55.6	51.0	25.7	26.1	27.3	27.3	26.6
	QUIK	43.7	68.0	71.3	73.3	40.0	75.7	45.1	64.6	60.2	34.7	40.6	39.8	31.8	36.7
	QuaRot	46.9	74.9	76.6	75.8	42.6	79.1	45.5	69.0	63.8	43.8	53.6	54.0	39.4	47.7
	SpinQuant	49.0	76.3	78.2	77.1	42.8	79.3	46.3	69.5	64.8	43.5	53.1	55.4	39.1	47.8
	ResQ	49.1	76.1	79.7	77.9	43.6	79.1	46.6	69.9	65.2	45.3	56.0	58.0	41.0	50.1
		Llama-3 family													
Model	Method	0-shot common sense reasoning tasks								0-shot MMLU tasks					
		ARC-c	ARC-e	BoolQ	HellaS	OBQA	PIQA	SIQA	WinoG	Avg.	humanities	Other	SocialS	STEM	Avg.
		(\uparrow)	(\uparrow)	(\uparrow)	(\uparrow)	(\uparrow)	(\uparrow)	(\uparrow)	(\uparrow)	(\uparrow)	(\uparrow)	(\uparrow)	(\uparrow)	(\uparrow)	(\uparrow)
Llama-3-8b	16-bit	53.2	77.1	81.1	79.2	44.8	80.9	47.0	73.4	67.1	55.0	70.6	73.2	53.7	63.1
	RTN	25.3	34.9	44.2	38.3	27.8	56.5	36.8	50.8	39.3	24.7	25.1	23.3	21.4	23.6
	GPTQ	24.7	37.7	44.3	36.8	27.0	57.6	36.4	53.8	39.8	24.7	23.9	22.8	21.8	23.3
	SmoothQuant+	27.5	42.0	50.7	44.9	28.8	59.0	35.9	50.9	42.5	25.4	25.5	24.5	23.4	24.7
	QUIK	33.6	56.4	60.5	61.5	33.2	68.7	39.9	59.0	51.6	30.0	34.0	34.8	32.1	32.7
	QuaRot	45.1	70.4	73.8	74.7	42.6	76.6	45.1	68.5	62.1	47.8	59.1	61.4	44.3	53.2
	SpinQuant	48.0	75.4	75.8	75.4	43.8	77.5	45.0	69.2	63.8	49.8	63.3	65.0	46.8	56.2
	ResQ	49.2	75.0	72.5	76.5	43.0	78.3	45.8	71.0	63.9	50.6	64.4	65.8	48.1	57.2
Llama-3-70b	16-bit	64.2	85.9	85.3	84.9	48.6	84.4	50.8	80.6	73.1	67.6	81.5	86.8	68.4	76.1
	RTN	32.6	50.3	54.2	41.3	31.6	64.8	35.9	53.2	45.5	24.5	23.8	22.3	22.1	23.2
	GPTQ	25.9	26.0	37.9	26.2	28.6	50.4	34.3	49.9	34.9	27.1	24.3	24.0	26.5	25.5
	SmoothQuant+	-	-	-	-	-	-	-	-	-	-	-	-	-	-
	QUIK	44.5	68.9	60.7	75.0	36.4	76.1	43.2	60.4	58.2	46.6	56.4	58.0	43.6	51.1
	QuaRot	53.7	74.5	81.6	81.1	46.6	81.0	46.8	75.2	67.6	55.7	72.5	75.8	57.3	65.3
	SpinQuant	52.0	77.3	81.7	75.6	43.8	78.8	43.4	72.8	65.7	50.7	67.0	68.1	51.9	59.4
	ResQ	61.4	84.3	83.9	83.5	46.0	83.1	48.6	78.3	71.1	64.9	79.9	84.9	66.1	74.0
		Llama-3.2 family													
Model	Method	0-shot common sense reasoning tasks								0-shot MMLU tasks					
		ARC-c	ARC-e	BoolQ	HellaS	OBQA	PIQA	SIQA	WinoG	Avg.	humanities	Other	SocialS	STEM	Avg.
		(\uparrow)	(\uparrow)	(\uparrow)	(\uparrow)	(\uparrow)	(\uparrow)	(\uparrow)	(\uparrow)	(\uparrow)	(\uparrow)	(\uparrow)	(\uparrow)	(\uparrow)	(\uparrow)
Llama-3.2-1b	16-bit	36.5	60.6	63.4	63.6	37.4	74.5	42.8	60.1	54.9	34.8	41.1	39.9	32.0	36.9
	RTN	22.4	29.9	53.4	31.4	29.4	54.8	34.9	48.5	38.1	24.8	25.2	22.4	22.7	23.8
	GPTQ	24.7	32.7	52.3	30.7	23.6	54.3	34.4	51.1	38.0	24.7	25.1	25.5	24.5	24.9
	SmoothQuant+	23.3	30.1	52.9	31.3	26.6	54.2	34.5	51.2	38.0	23.9	24.1	25.0	23.5	24.1
	QUIK	27.4	46.0	55.0	46.0	26.4	62.4	38.6	52.6	44.3	25.6	25.6	24.6	24.5	25.1
	QuaRot	30.0	51.4	59.1	54.0	34.2	66.7	39.6	57.1	49.0	25.4	26.9	25.4	24.4	25.5
	SpinQuant	32.3	51.8	59.3	55.4	30.4	67.7	38.6	54.7	48.8	25.4	27.6	24.2	25.3	25.6
	ResQ	34.0	54.2	57.0	57.3	31.2	69.4	41.0	56.8	50.1	28.3	30.5	31.3	27.6	29.4
Llama-3.2-3b	16-bit	46.2	71.7	73.1	73.7	43.4	77.4	47.2	69.1	62.7	48.9	62.9	62.3	45.2	54.8
	RTN	23.5	35.4	46.2	35.6	28.2	56.3	33.6	50.6	38.7	25.1	25.6	27.0	24.9	25.7
	GPTQ	27.0	27.0	48.8	44.4	27.8	59.1	37.1	51.5	40.3	24.9	24.5	25.7	24.0	24.8
	SmoothQuant+	25.3	33.1	47.8	37.7	25.2	56.2	35.8	50.9	39.0	25.4	26.6	26.4	25.3	25.9
	QUIK	32.9	50.1	52.6	59.1	33.2	68.7	40.3	53.0	48.8	29.0	33.2	31.9	30.3	31.1
	QuaRot	38.6	59.0	65.9	66.5	35.8	74.4	43.1	65.2	56.1	38.5	47.3	46.7	35.3	42.0
	SpinQuant	38.9	64.8	68.0	69.1	39.4	74.9	45.1	62.9	57.9	37.0	49.4	50.5	39.9	44.2
	ResQ	43.1	65.6	68.8	70.5	38.4	75.1	45.6	64.8	59.0	44.7	57.0	56.5	41.0	49.8

Table 5: Accuracy on eight 0-shot common sense reasoning tasks including ARC-challenge, ARC-easy, BoolQ, HellaSwag, Openbook QA, PIQA, SIQA, and WinoGrande and 0-shot massive multitask language understanding tasks across four subjects: STEM, Humanities, Social Sciences, and MMLU-other, for the Llama-2, Llama-3 and Llama-3.2 families when quantized to W/A/KV = 4/4/4. Results of all techniques were obtained using their official codebase. Our work ResQ and QUIK (Ashkboos et al., 2023) keep $1/8$ th of channels in 8-bit. All techniques except RTN use GPTQ (Frantar et al., 2022).

$P_l P_l^\top + P_h P_h^\top = I$, we have

$$\begin{aligned}
\|X - X_q\|_F &\leq \frac{\sqrt{\log(d-r)\pi}}{2^{L-1}-1} (\mathbb{E}\|X\|_F - \mathbb{E}\|X P_h\|_F) \\
&+ \frac{\sqrt{\log(r)\pi}}{2^{H-1}-1} \mathbb{E}\|X P_h\|_F \\
&= \frac{\sqrt{\log(d-r)\pi}}{2^{L-1}-1} \mathbb{E}\|X\|_F \\
&- \left(\frac{\sqrt{\log(d-r)\pi}}{2^{L-1}-1} - \frac{\sqrt{\log(r)\pi}}{2^{H-1}-1} \right) \mathbb{E}\|X P_h\|_F
\end{aligned} \tag{12}$$

Since $\frac{\sqrt{\log(d-r)\pi}}{2^{L-1}-1} - \frac{\sqrt{\log(r)\pi}}{2^{H-1}-1} > 0$ the quantization error is reduced by maximizing $\|X P_h\|_F$

A.2 Distribution of activations

The distribution of activations after projection by U is shown in Figure 6. The formulation of U ensures that the final r channels in the activation map comprise of coefficients along basis vectors with maximum activation variance. Consequently, keep

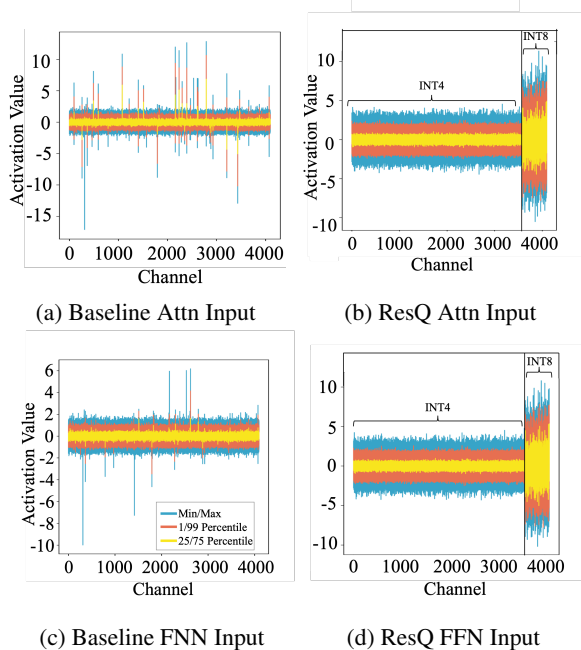


Figure 6: Input activation distributions of attention and FFN layers, for baseline (a and c) and ResQ (a and b).

	Quarot	ResQ	SpinQuant
Llama-3.2-1b	4m	7m	13m
Llama-3.2-3b	8m	16m	38m
Llama-3-8b	17m	35m	1h41m
Llama-2-7b	15m	33m	1h37m
Llama-2-13b	23m	1h	3h42m

Table 6: Time taken (in NVIDIA A100 GPU hours) to quantize the model. All approaches use GPTQ for weight quantization. SpinQuant uses 4 GPUs to optimize rotation matrices.

those channels in high precision minimizes quantization error. The remaining channels are more amenable to quantization due to the application of random rotations which suppress outlier values.

A.3 Complete results of main result tables

Task by task results of the Table 1 in main paper is shown in Table 5. As expected, ResQ achieves su-

perior performance than baselines across the series of common sense reasoning and MMLU tasks.

A.4 Additional implementation details

In this work, obtaining the projection matrices and quantization of weights for **all the models** is performed on a single NVIDIA A100 80GB GPUs. Time taken by ResQ compared with other approaches is shown in Table 6. Evaluation on various benchmarks for all the models is also done on a single NVIDIA A100 GPU with the sole exception of Llama-3-70b which requires 4 GPUs for evaluation. We use `lm_evaluation_harness` version 0.4.5 (Gao et al., 2024) and LongBench (Bai et al., 2024) for all the evaluation tasks. For Arc-c/e, Hellaswag, OpenBook QA, PIQA tasks we report `acc_norm` while for BoolQ, SIQA and Winogrande we report `acc`.

For calibration data, we use 512 randomly chosen samples for Wikitext to obtain the projection matrices. While for GPTQ we use 128 randomly chosen samples from Wikitext following the original work (Frantar et al., 2022).

The KV cache, as well as the weights and activations of all Linear layers (except `mlp.down_proj`), are quantized to 4-bit precision, with $\frac{1}{8}$ of channels retained in 8-bit precision. While, the weights and activations within `down_proj` are uniformly quantized to 4-bit precision. Following (Ashkboos et al., 2024b) and (Liu et al., 2024a), we keep query vector in 16-bit.

A.5 Artifact licences

According to their licenses, all language models used in the paper fall under acceptable use case. The licenses for the models are linked for perusal : [Llama-2-7b](#), [Llama-2-13b](#), [Llama-3-8b](#) and, [Llama-3-70b](#), [Llama-3.2-1b](#), [Llama-3.2-3b](#).